Optical Measurements of Muzzle Blast

E. M. Schmidt* and D. D. Shear†
U. S. Army Ballistic Research Laboratories, Aberdeen Proving Ground, Md.

The structure of the flowfields formed about the muzzle of a small caliber rifle during the firing are measured using a time-resolved, spark shadow-graph technique. The initial flow from the muzzle occurs as tube gases are forced out ahead of the projectile. The gas is air and the exit properties are $V_e = 945$ m/sec, $M_e = 1.48$ and $P_e/P_\infty = 15$. A second flowfield forms upon separation of the projectile which releases the propellant gases. After an initial, in-bore expansion, the propellant gas muzzle properties are $V_e = 1295$ m/sec, $M_e = 1.0$, and $p_e/p_\infty = 600$. While the exit properties are different, the flowfields develop in a similar manner. In the axial or downrange direction, strong coupling between the jet and blast fields is observed; however, along the lateral boundaries, the coupling is very weak with the jet structure remaining invariant once established. Motion of observable discontinuities along the axis of symmetry is shown to qualitatively agree with variable energy blast wave theory. At late times, the air blast and jet flows are shown to uncouple and decay independently.

Nomenclature

D = reference dimension (gun caliber)
M = Mach number
p = pressure
R = gas constant
T = temperature
t = time
V = velocity
X = axial distance from muzzle
Y = lateral distance from axis of symmetry
γ = ratio of specific heats
τ = time scale of precursor flow

Superscript

$*$ = sonic conditions

Subscripts

e = muzzle exit conditions
∞ = ambient conditions

Introduction

MEASUREMENTS of the structure of impulsive supersonic jets and associated free-air disturbances have generally been qualitative in nature[1] or limited to time-displacement histories of the motion of selected observable discontinuities along the axis or plane of symmetry.[2-4] Since such flows are generated in thruster and retro-rocket firings, silo ejections, shock tunnel discharges, and launching tube-fired projectiles, quantitative investigation of the development and decay of the overall jet and air blast structures is of interest. This paper presents the results of a detailed study of the flowfield about the muzzle of a small caliber rifle during firing.

In firing tube launched projectiles, two impulsive jet flows are generated, Fig. 1. The first, or precursor, flowfield develops as the air residing in the tube ahead of the projectile is forced out by the projectile motion. The second, or propellant gas, flowfield develops when the high-pressure gases are released by projectile separation from the launcher. Generally, the propellant gases are highly energetic and rapidly expand through the precursor flowfield, effectively destroying it. Both flows exhibit the structure of a supersonic, underexpanded jet encapsulated within a nearly spherical blast. At early times, the blast field constrains the development of the jet. The decay of the blast due to spherical expansion removes this constraint permitting the flow to expand freely. In guns, subsequent variations in the exhaust jet structure are dominated by the decreasing muzzle pressure as the tube empties.

Cranz[1] reports using spark schlieren techniques to obtain photographs of the muzzle gas flowfield about a rifle as early as 1911. The sequences of photographs produced show the development of the precursor and propellant gas flowfields. However, the data acquisition technique did not permit accurate resolution of the time base. Buckmaster[2] uses schlieren and photomultiplier observations of shock luminosity to examine the impulsive expansion from a slit nozzle. The observed motion of the blast wave is shown to follow a power law in time which agrees well with strong blast theory. The details of the developing jet structure and off axis shock motion were not addressed. Starshinov[3] and Naboko[4] investigate both cylindrical and axially symmetric flows in studies again directed to the flow along the axis of symmetry.

Using the method of characteristics, Oswatitsch[5] models the muzzle flowfield as a spherical blast. His results show that in the region between the muzzle and the inward facing shock, temporal variations in flow properties occur at a rate proportional to changes in the muzzle conditions. Since these changes occur gradually relative to the time scale of the blast field growth, Oswatitsch concludes that between the muzzle

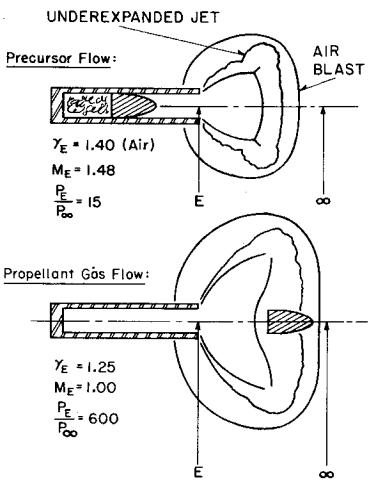

Fig. 1 Muzzle flows.

Presented as Paper 74-531 at the AIAA 7th Fluid and Plasma Dynamics Conference, Palo Alto, California, June 17-19, 1974; submitted September 26, 1974; revision received January 21, 1975.

Index categories: Shock Waves and Detonations; Jets, Wakes, and Viscid-Inviscid Flow Interactions.

*Aerospace Engineer, Exterior Ballistics Laboratory. Associate Member AIAA.

†Physical Science Technician, Exterior Ballistics Laboratory.

and Mach disk the gun exhaust may be modeled as a steady jet.

While Oswatitsch uses this steady approximation to estimate loading on certain categories of projectiles, he can not treat certain important features of the muzzle gas flow. Among them are the effects of initial propellant gas expansion between the base of the projectile and the muzzle rim and the effects of interactions between the precursor and propellant gas flows. Since these features occur near the muzzle where gas pressures are maximum, a more exact treatment of this portion of the problem would appear justified. Recently, a number of attempts[6-8] have been made to apply finite-difference techniques to the calculation of the properties of these type flows. The calculations are capable of predicting the development of the muzzle gas flow in great detail; however, the accuracy and validity of these calculations must be compared with experiment.

At present, the body of quantitative data relating to muzzle blast is extremely limited. This paper presents the results of an experimental survey of the muzzle flow about a 5.56mm, M-16 rifle. A time-resolved, spark shadowgraph technique is used to construct detailed trajectories of observable discontinuities. Observations are presented not only of the flow along the axis of symmetry but also of the lateral boundaries. Data are taken over the complete firing cycle showing both the growth and decay of the exhaust plume.

Experimental Apparatus and Test Techniques

Data was taken about the muzzle of an M-16 rifle firing ball ammunition. The weapon has a nominal muzzle diameter of 5.56mm, a barrel length of 470mm, and a twist of rifling of 1 turn in 305mm. The ammunition fired was from a single lot, number FA 565. The projectile was ball, M-193 weighing 54.1 grains with a length of 19.1mm. The propellant was 27.5 grains of WC 846. A muzzle velocity of 945 m/sec was measured using the equipment described in this section.

Since data is obtained optically, a technique is used which minimizes overexposure from muzzle flash. Of the several optical arrangements available,[9] a spark shadowgraph system is used which incorporates a Fresnel lens to reduce object luminosity, Fig. 2. The gun is located on the same side of the Fresnel lens as the spark light source; however, while the spark is beyond the focal point, the gun is between the focal point and the lens. In this manner, the light from the source is focused at a point on the opposite side of the lens while the luminosity from the object of interest is diffused away. An open shutter camera is positioned with its objective lens at the source image point and is focused on the plane of the Fresnel lens. Thus, shadowgraphs are taken which use the spark duration to provide stop-action but do not suffer from overexposure. This optical arrangement is particularly well suited for adoption of a multiple exposure technique, the Cranz-Schardin[9] method. An array of spark sources on one side of the lens is focused on the objective lenses of a complementary array of cameras on the opposite side. The number of photographs taken in this manner is limited by the geometry and physical dimensions of the spark and photographic equipment and by the dimensions and quality of the main lens. In these experiments, three sequential photographs at preselected time intervals are obtained from each firing.

To construct a time-displacement history of observable discontinuities, a test technique is used which gives a reliable time base to the sequence of three photographs and permits the correlation of data from various firings. The basic assumptions of the technique are that the projectile velocity is constant during its travel through the muzzle gases and that the projectile velocity is consistent from shot to shot. Once these assumptions are made, it is necessary to insure that at least one photograph in each sequence of three contains an image of the projectile. By measuring the distance between the projectile base and the muzzle of the gun, a reference distance

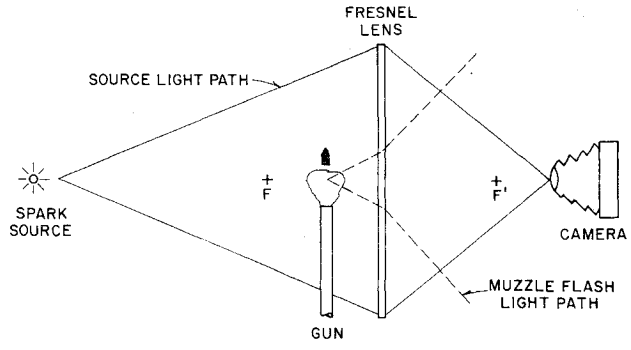

Fig. 2 Schematic of optical arrangement.

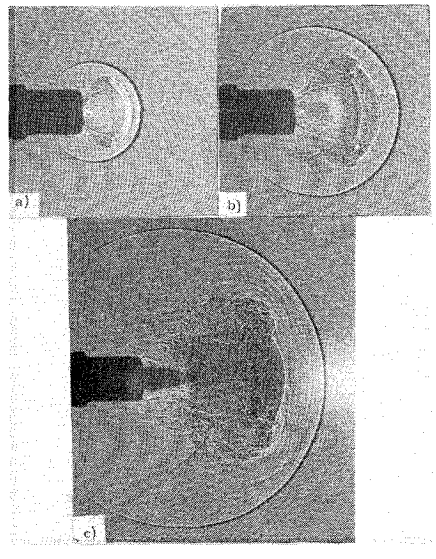

Fig. 3 Precursor flow development: a) $t = -78$ μsec; b) $t = -50$ μsec; and c) $t = -5$ μsec.

is obtained. This distance is divided by the measured muzzle velocity to obtain a reference time for the baseline photograph of the sequence. Once the reference time for one photograph of the sequence is obtained, it is a simple matter to use the measured intervals between spark firings to obtain the time of each photograph.

Results

Precursor Flow Development

The precursor flow forms as tube gases are pushed out of the gun bore by the moving projectile. These gases are composed of air and residual and leaked propellant gases. Since the current tests involved single firings with relatively long times between shots, the amount of residual propellant gases present in the gun tube is minimal. Additionally, for the weapon considered in these studies, leakage is not significant and will be neglected.

As the projectile accelerates, compression waves move ahead of it into the tube air. These waves coalesce to form a shock which continually increases in strength as more waves intercept it. This variation in strength implies that entropy gradients exist in the slug of accelerated tube air. Oswatitsch[5] points out that an adequate approximation of the properties of the gas slug at the muzzle can be obtained using the Rankine-Hugoniot relations under the assumption that the gas velocity is equal to the projectile launch velocity. He bases this upon the fact that for high-speed projectiles, the most significant accelerations occur near the breech leaving the projectile velocity relatively constant over most of the latter portion of its in-bore trajectory. For a projectile launch velocity of 945 m/sec, this approximation predicts an exit

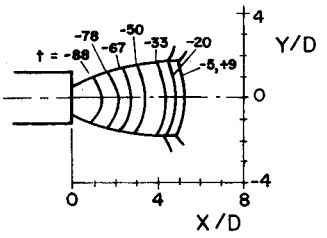

Fig. 4 Precursor jet shock contours (t in μsec).

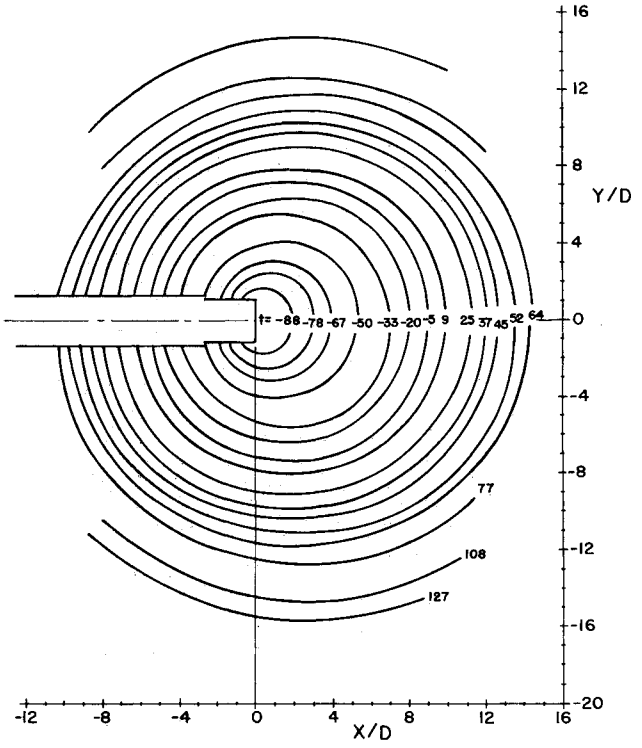

Fig. 5 Precursor air blast contours (t in μsec).

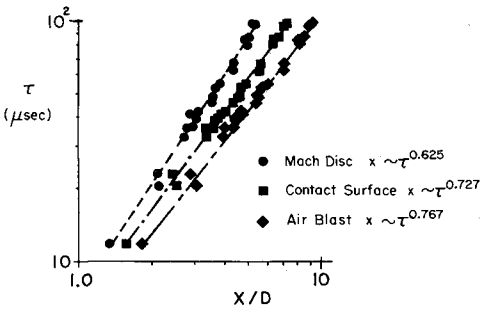

Fig. 6 Precursor flow axial discontinuity trajectories ($\tau = t + 100$).

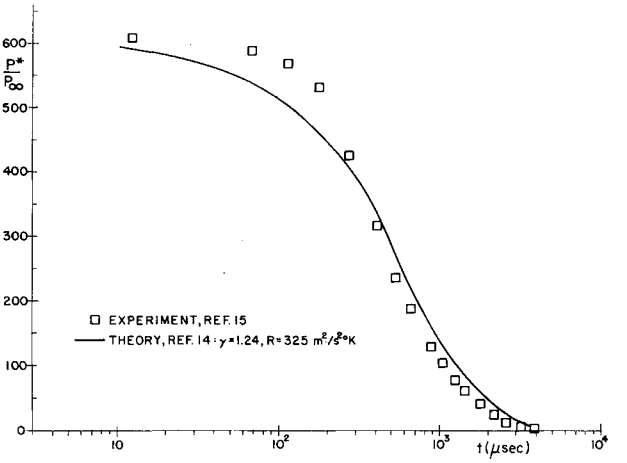

Fig. 7 Propellant gas pressure at muzzle ($M_e = 1.0$).

static pressure of 15 atm, Mach number of 1.48, and a shock velocity of 1240 m/sec.

A set of spark shadowgraphs of the precursor flow development is shown in Fig. 3. For the data shown throughout this paper, zero time is taken as the instant when the projectile base passes the muzzle of the gun. Thus, in the precursor flow, times referenced to this baseline are negative. The data commence 20 μ sec after the precursor shock separates from the tube.

As the precursor gas flows from the muzzle, it expands two-dimensionally forming an underexpanded, supersonic jet. The growth of the precursor jet displaces the surrounding air generating a nearly spherical blast. The development of this type flow has been examined in connection with shock propagation from the open end of shock tubes.[2-4] These studies show the initial expansion of the gas to be quite complex. Two-dimensional, unsteady expansions propagate into the flow from the edge of the muzzle and move along the shock front turning the flow behind it away from its purely axial direction. In the tube gases, these waves form the stationary wave structure of the underexpanded jet; however, within the shock layer between the Mach disk and air blast, highly unsteady conditions persist throughout the period of observation.

The contact surface separates the gas which originally was in the gun from that which was external to it. On the lateral boundaries, the large tangential velocity difference between the two flowfields generates significant viscous effects as evidenced by the strong turbulence along these surfaces and the presence of a vortex ring formed upon the intrusion of the tube gases into the atmosphere. In the forward or downrange direction, the contact surface takes the form of a spherical cap indicating a total absence of shear. While the contact surface is the expanding boundary of the tube gas jet which drives the free-air blast, it is also the boundary at which the jet structure adjusts to changes in the properties of the blast layer. Thus, assuming that the muzzle exit properties are nearly constant, variations in the contact surface with time should give an indication of the strength of interaction between the jet and blast fields. However, in the shadowgraphs, the turbulent nature of this surface make it the most difficult of the observable discontinuities to accurately locate. The tube gas jet shock structure is much more clearly defined.

Analyses[10,11] of steady free jets show that the shock structure of a supersonic, underexpanded jet represents the locus of inwardmost propagation of disturbances from the jet boundaries. Thus, the shock structure of the precursor tube gas jet will be responsive to variations in the blast field, and, due to its high degree of visibility, serve as an excellent indicator of the nature of jet/blast coupling. A plot of the jet shock structure over the period of observation is shown in Fig. 4. The most apparent feature of the shock structure is the invariant nature of the intercepting shock location once established behind the Mach disk indicating that pressure levels in the lateral portion of the blast field rapidly decrease to a nearly constant value (ambient) soon after the precursor flow commences. Since the muzzle exit conditions are nearly constant, this demonstrates the existence of quasi-steady, jet flow within the grossly unsteady muzzle blast. The presence of a quasi-steady core flow was predicted analytically by Oswatitsch.[5]

To account for the motion of the Mach disk, an analysis of the shock layer is required. A contour plot of the developing precursor blast, Fig. 5, shows the blast to be quite spherical in nature. In fact, examination of the spark shadowgraphs, Fig. 3, indicates that the Mach disk, contact surface, and blast form nearly concentric spherical surfaces. Such a configuration is strongly suggestive of the applicability of blast theory to this portion of the flowfield. Further confirmation

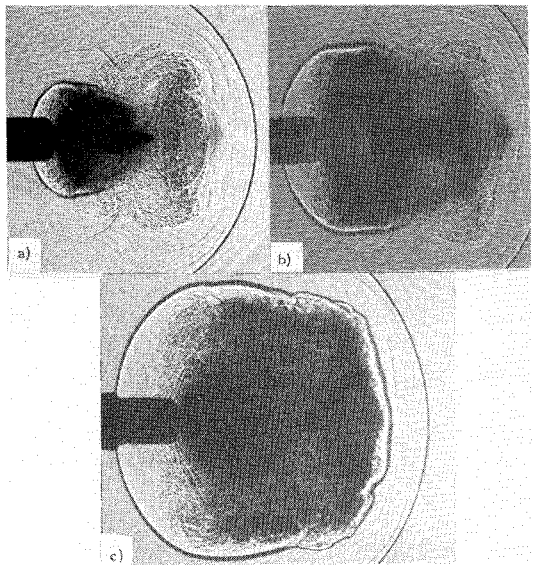

Fig. 8 Propellant gas flow development: a) $t=9$ μsec; b) $t=25$ μsec; and c) $t=37$ μsec.

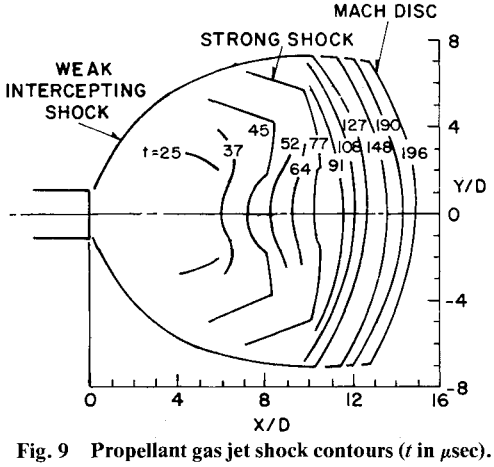

Fig. 9 Propellant gas jet shock contours (t in μsec).

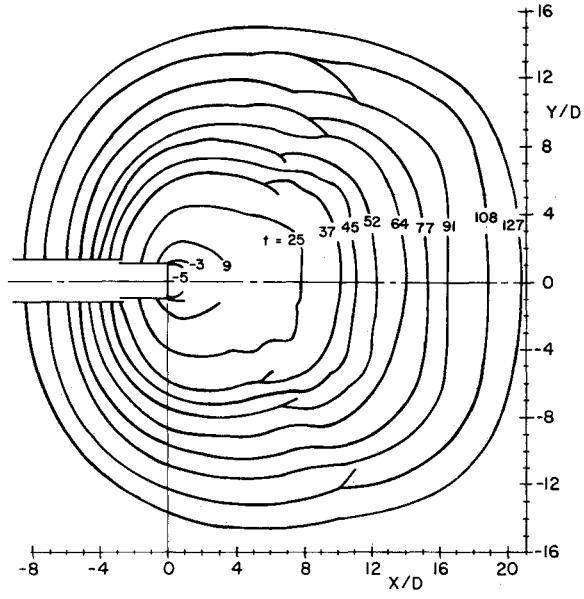

Fig. 10 Propellant gas air blast contours (t in μsec).

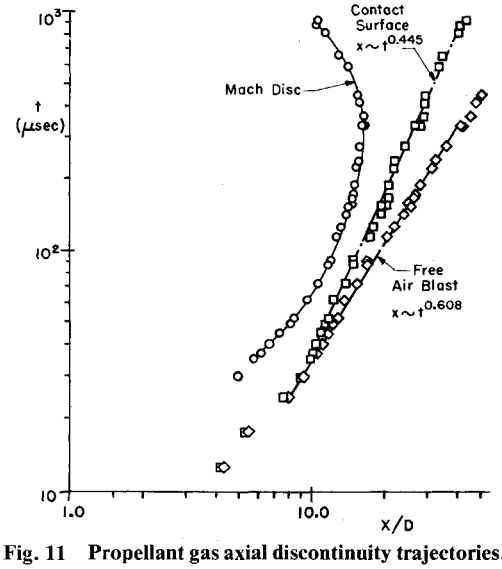

Fig. 11 Propellant gas axial discontinuity trajectories.

of this tendency is indicated by plotting the motion of these discontinuities along the axis of symmetry, Fig. 6. The data is plotted against a time scale commencing when the precursor shock first breaks the muzzle at roughly -100 μ sec. The data is seen to follow a power-law variation in time typical of the predictions of blast wave theory.[12]

Propellant Gas Flow Development

Ejection of the projectile releases the propellant gases to expand through the precursor flow into the atmosphere. These gases[13] are a complex mixture of oxides of nitrogen, carbon and sulfur, water vapor, and organic compounds; however, Celmins[14] treats them as a perfect gas to compute the interior ballistics of the M-16 both prior and subsequent to shot ejection. While the projectile is in-bore, the high temperature of the propellant gases, $T\cong 2500$ K, results in a subsonic Mach number, $M=0.7$, behind the projectile. Thus, at shot ejection, an expansion propagates into the gun tube producing a sonic muzzle condition which is maintained until the gun is nearly empty. The calculated pressure delay at this sonic orifice, Fig. 7, compares favorably with measured values.[15]

The sudden change in muzzle properties at shot ejection is clearly indicated in the spark shadowgraphs, Fig. 8. The increased muzzle pressure, $p_e/p_\infty=600$, and decreased ratio of specific heats, $\gamma=1.24$, produce a jet with an initial expansion angle and overall geometry significantly larger than the precursor jet. The rapid expansion of the propellant gases through the lateral boundaries of the precursor jet and into the relatively quiescent atmosphere generates a strong blast; however, in the forward direction, the existence of the high velocity precursor jet core delays formation of a strong blast until the propellant gases penetrate the Mach disk of the precursor jet, $t=25$ μsec.

While partially obscured by particulate propellant residue, the developing jet shock structure may be extracted from the spark shadowgraphs, Fig. 9. The Mach disk moves continuously away from the muzzle leaving behind an intercepting shock structure which remains invariant once established. Since the muzzle pressure is nearly constant over the initial 200 μsec, the invariant nature of the intercepting shock structure indicates the weakness of interactions with the lateral blast field. The shock contours from 25 through 100 μsec show the simultaneous appearance of three types of shocks. Weak oblique, strong oblique, and normal shocks appear successively in following the shock structure from the muzzle to the axis of symmetry. The data indicate that while the projectile locates the position of the normal shock on the axis, the off-axis Mach disk structure forms due to interaction between the jet and blast fields. After 91 μsec, the projectile no longer affects the internal shock structure of the jet.

Growth of the air blast formed by the propellant gases is shown in Fig. 10. Because of leakage around the boattail of

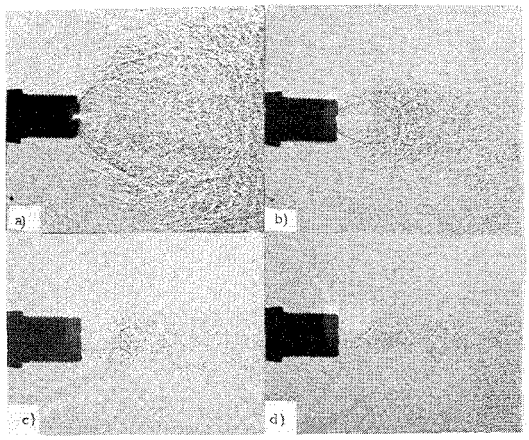

Fig. 12 Propellant gas decay sequence: a) $t = 900$ μsec; b) $t = 3200$ μsec; c) $t = 4200$ μsec; and d) $t = 5200$ μsec.

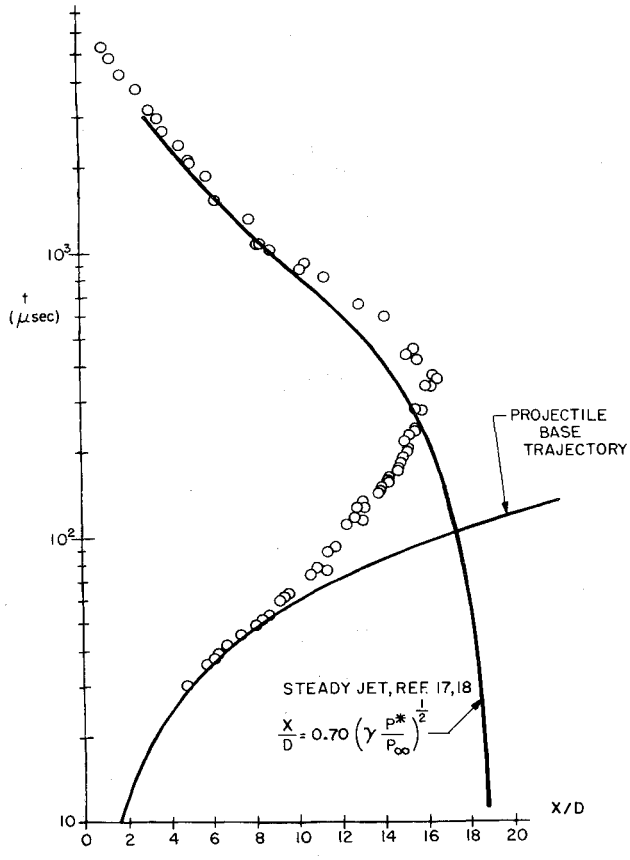

Fig. 13 Propellant gas jet axial Mach disk trajectory.

the projectile, the blast formation precedes the separation of the projectile base. Near the muzzle, the development of the blast wave is affected both by the presence of the projectile and by interactions with the precursor flow; however, after the first 10 μsec, the flow begins to expand freely. Subsequently, the blast strength is seen to be greatest in the downrange direction reflecting the directed nature of energy deposition. The propellant blast continues to maintain its downrange strength for a considerably longer period than did the precursor gas. Only as it passes from the field of view, does the blast begin to exhibit a roughly spherical nature.

The motion of observable discontinuities along the axis of symmetry is shown in Fig. 11. As a result of interactions with the projectile at early time and decay of muzzle properties at later times, the motion of the Mach disk does not appear to follow a power-law variation; however, the motion of the contact surface and blast both follow power laws in time. The strong blast analysis of Freeman[12] shows that a spherical blast propagating at the measured power law, $X \sim t^{0.608}$, requires a nearly constant rate of energy input, $\dot{E} \sim t^{0.04}$. Celmins[14] shows that during the first 100 μsec the rate of energy efflux from the muzzle is proportional to $t^{-0.04}$. Based on this strong correlation between observed and predicted blast motion, Erdos and Del Guidice[16] construct a finite-difference model of the flow assuming spherical symmetry near the axis. The resulting computations of the complete flowfield between the muzzle and the blast wave show excellent agreement with the present observations.

The preceding data indicate that the initial expansion of the propellant gases is dominated by the developing air blast. The pressure behind the blast propagating along the axis decays from an estimated overpressure of 120 atm at the muzzle to 1.3 atm, based on the blast wave velocity at 200 μsec. Thus, the axial motion of the Mach disk and contact surface is most sensitive to the two-order-of-magnitude variation in blast overpressure compared against a muzzle pressure decay from 600 to 450 atm in the same period. The lateral structure of the jet is observed to be invariant over this time for two reasons. First, the lateral blast field over pressure decays rapidly since it is not directly driven by the expanding gases; i.e., along the forward contact, the blast and jet velocity vectors are nearly colinear. While along the lateral boundaries, the velocities of the inviscid flows are nearly orthogonal. Second, steady flow calculations[10,11] show underexpanded jet structure is relatively insensitive to small variations in pressure ratio for $p_e/p_\infty > 200$.

Propellant Gas Flow Decay

This phase of the muzzle flow has the longest duration, from 200 μsec to flow termination at approximately 6000 μsec. The nature of the decay is opposite to the development; namely, the blast field has a secondary influence compared to the decreasing muzzle pressure. At 200 μsec, the overpressure behind the blast has a maximum of 1.3 atm. Continued radial expansion of the blast decreases the pressure sensed by the jet to ambient values prior to 1000 μsec. The decrease of muzzle pressure from 450 atm to ambient dominates the decay of at least the supersonic core of the propellant gas jet.

The stages of jet decay are shown by the spark shadowgraphs to be markedly different from its growth, Fig. 12. Whereas the jet grew in the axial direction within the lateral boundaries of a constant (exit) property jet, its decay displays a complete collapse of the shock structure. As the jet shrinks toward the muzzle, the photographs capture the flow patterns of underexpanded jets with continually decreasing pressure ratio. The final shadowgraph, $t = 5200$ μsec, displays the repeating shock structure typical of a weakly underexpanded jet.

An indication of the correspondence between the instantaneous structure of the muzzle jet and a steady jet with identical exit properties may be obtained from a comparison of Mach disk location, Fig. 13. The steady state Mach disk location is based on an empirical relation,[17,18] which for sonic exit conditions is:

$$X/D = 0.70\ (\gamma p^*/p_\infty)^{1/2}$$

with the pressure ratio determined at each instant by the analysis of Celmins,[14] Fig. 7. After an initial period of attachment to the projectile, the Mach disk separates and attains a maximum standoff at 400 μsec. The data overshoots the corresponding steady-state location apparently responding to subatmospheric pressures typical of overexpansions behind spherical blasts. The occurrence of maximum Mach disk standoff and optimal jet size does not correspond. After 200 μsec, the Mach disk is pulled outward by the blast field overexpansion, while the lateral jet boundaries begin to shrink due to decreasing muzzle pressure and relatively constant external pressure. Recovery of the axial blast field pressure to

ambient gradually reduces the Mach disk overshoot until agreement with the steady state correlation is achieved at 800 μsec.

The behavior of the jet structure at late times indicates the flow experiences a period of transition, 200 μsec$\rightarrow$800 μsec, in which the influence of the blast field on the jet continually diminishes and the decaying muzzle pressure assumes dominance. Subsequent to 800 μsec, the jet structure is completely determined by the muzzle properties and is adequately represented as an instantaneously steady jet.

Conclusions

Optical techniques were used to construct accurate time-displacement records of the two distinct flowfields generated at the muzzle of a gun during firing. Both flows are shown to develop the structure of impulsively generated, underexpanded jets. This occurs in fundamentally identical manners even though the muzzle exit properties are dissimilar. The precursor flow precedes the projectile, exiting the muzzle at a supersonic velocity and moderately underexpanded state. The propellant gas flow follows the projectile with a sonic muzzle velocity and large overpressure.

In both cases, the observed structure is composed of two interacting flowfields; an underexpanded, tube gas jet and a free-air blast. The development of the jet structure occurs anisotropically. In the axial or forward direction, the jet Mach disk and tube gas-air interface grow continually; however, during this same period, the lateral jet boundaries remain invariant once established. Since the muzzle properties are relatively constant through this stage, the anisotropic behavior is directly related to the variation in blast field strength around the jet periphery. In the forward direction, a strong blast is generated; while in the lateral directions, the blast is weak and decays rapidly. The growth of discontinuities along the axis follows power laws in time which are shown to agree with the values predicted by strong blast theory.

Decay of the propellant gas jet exhibits two stages. First, a transition period is noted in which the influence of the decaying blast field diminishes and variations in muzzle properties assume greater importance. The final stage shows the supersonic core of the jet collapsing toward the muzzle. During this collapse, deterioration of the muzzle pressure is dominant, and the data show that steady-state theory adequately predicts the instantaneous jet structure.

References

[1] Cranz, C. and Glatzel, B., "Die Ausstromung von Gasen Bei Hohen Afangsdrucken," *Annalen der Physik* (Leipzig), Vol. 43, 1914, pp. 1186-1204.

[2] Buckmaster, J. D., "An Investigation of Cylindrical Starting Flows," *AIAA Journal*, Vol. 2, Sept. 1964, pp. 1649-1650.

[3] Starshinov, A. I., "Experimental Investigation of the Initial Stage of the Formation of a Gas Jet," *Mekhaniki Astronomii*, No. 3, May 1964, pp. 110-113.

[4] Naboko, I. M., Bazhenova, T. V., Opara, A. I., and Belavin, V. A., "Formation of a Jet of Shock-Heated Gas Outflowing into Evacuated Space," *Astronautica Acta*, Vol. 17, Oct. 1972, pp. 653-658.

[5] Oswatitsch, K., "Intermediate Ballistics," DVL Rept. 358, June 1964, Deutschen Versuchsanstalt fur Luft-und Raumfahrt, Aachen, Germany.

[6] Taylor, T. D., "Calculation of Muzzle Blast Flow Fields," CR 4155, Dec. 1970, Picatinny Arsenal, Dover, N.J.

[7] Ishiguru, T., "Finite-Difference Calculations for Two-Dimensional Unsteady Expanding Flows, *AIAA Journal*, Vol. 10, Feb. 1972, pp. 217-218.

[8] Traci, R. M., Farr, J. L., and Liu, C. Y., "A Numerical Method for the Simulation of Muzzle Gas Flows with Fixed and Moving Boundaries," BRL CR 161, June 1974, Ballistic Research Labs., Aberdeen Proving Ground, Md.

[9] Hyzer, G., *Photographic Instrumentation: Science and Engineering*, 1st ed., U.S. Government Printing Office, Washington, D.C., 1965.

[10] Love, E. S., Grigsby, C. E., Lee, L. P., and Woodling, M. J., "Experimental and Theoretical Studies of Axisymmetric Free Jets," TR R-6, 1959, NASA.

[11] Vick, A. R., Andrews, E. H., Dennard, J. S., and Craidon, C. B., "Comparison of Experimental Free-Jet Boundaries with Theoretical Results obtained with the Method of Characteristics," TN D-2327, June 1964, NASA.

[12] Freeman, R. A., "Variable-Energy Blast Waves," *British Journal of Applied Physics (Journal of Physics, D)*, Ser. 2, Vol. 1, 1968, pp. 1697-1710.

[13] Rocchio, J. J. and May, I. W., "Analysis of Exhaust Gases from the XM-19 Rifle—An Application of Gas Chromatography/Mass Spectroscopy," BRL MR 2293, May 1973, Ballistic Research Labs., Aberdeen Proving Ground, Md.

[14] Celmins, A., "Theoretical Basis of the Recoilless Rifle Interior Ballistic Code, RECRIF," Ballistic Research Labs., Aberdeen Proving Ground, Md., to be published.

[15] Brosseau, T. L., "Interior Ballistics Study of the M16A1 Rifle," BRL MR 2190, May 1972, Ballistic Research Labs., Aberdeen Proving Ground, Md.

[16] Erdos, J.I. and Del Guidice, "Gas Dynamics of Muzzle Blast," *AIAA Journal*, Vol. 13, Aug. 1975, pp. 1048-1055.

[17] Lewis, C. H. and Carlson, D. J., "Normal Shock Locations in Underexpanded Gas and Gas-Particle Jets," *AIAA Journal*, Vol. 2, April 1964, pp. 776-777.

[18] Werle, M. J., Shaffer, D. G., and Driftmeyer, R. T., "Freejet Terminal Shocks," *AIAA Journal*, Vol. 8, Sept. 1970, pp. 2295-2297.